DOI: 10.1021/ma902625p

Macromolecules
COMMUNICATION TO THE EDITOR

Differences Between Crystals Obtained in PLLA-Rich or PDLA-Rich Stereocomplex Mixtures

Damien Maillard[†,‡] **and Robert E. Prud'homme***[,†]

[†]*Département de chimie, Université de Montréal, Succursale Centre-Ville, C.P. 6128, H3C 3J7 Montréal, Qc. Canada*
[‡]*Present address: Department of Chemical Engineering, Columbia University, New York, NY 10027.*

Received November 30, 2009
Revised Manuscript Received March 12, 2010

Introduction. One of the fascinating observations with semicrystalline polymers is that of banded spherulites caused by the twisting of the lamellae. Many polymers exhibit this behavior upon crystallization, including polyethylene.[1−4] Because polyethylene is a linear nonchiral polymer that crystallizes in a flat zigzag chain conformation, the origin of the twisting has been the subject of numerous studies and several theories.[5−13] One of these theories describes a lamella as being made of two half-lamellae bending in opposite directions; the linkage of these two half-lamellae leads to the twisting of the complete lamella.[14−18] Keith et al. have been able to observe half-lamellae in ultrathin films of polyethylene and to show their curvature.[19]

In the specific case of polylactides, we have previously shown that the chirality of the chain dictates the sense of curvature of the edge-on lamellae observed in ultrathin films (10−60 nm in thickness).[20,21] Those edge-on lamellae can be considered to be half-lamellae, and their sense of curvature is related to the sense of twisting of the complete lamellae. The presence of the substrate in ultrathin film crystallization actually provokes the atrophy of one-half of the lamella, reducing its twist to a curvature. In the case of poly(L-lactide) (PLLA), the complete lamella is right-handed twisted and the half-lamella is S-shaped, whereas, in the case of poly(D-lactide) (PDLA), the complete lamella is left-handed and the half-lamella is Z-shaped. To the best of our knowledge, this is the first example of synthetic polymers of a chirality transfer from the chain to the curved lamella (or half-lamella) in ultrathin films and from this curved half-lamella to the twisted complete lamella inside the spherulite, although several similar examples have been reported for natural macromolecules.[22,23]

If the two isotactic polyenantiomers of polylactides are blended together, they form a crystalline stereocomplex whose properties greatly differ from those of PLLA and PDLA taken separately. For example, the melting temperature is increased by 50 °C (from 180 to 230 °C), and the crystalline structure shifts from an orthorhombic unit cell (stable α modification, $a = 1.078$, $b = 0.604$, and $c = 2.873$ nm)[24] to a triclinic ($a = b = 0.916$, $c = 0.870$ nm, $\alpha = \beta = 109.2°$, $\gamma = 109.8°$, two chains per cell)[25] or trigonal ($a = b = 1.498$ nm, $c = 0.870$ nm, $\alpha = \beta = 90°$, $\gamma = 120°$, six chains per cell)[26] unit cell. The triclinic and trigonal unit cells actually describe the same chain packing, in which the two enantiomers are included in the crystal with the same helical pitch (3_1) but in opposite directions, left-handed in the case of PLLA and right-handed in the case of PDLA. This unit cell can be considered as "racemic", made of the two enantiomeric forms of polylactide, that is, a nonchiral crystal generated by the blend of two chiral polymers.

Chiral small molecules that exhibit opposite asymmetric crystallization behavior when taken separately can often form racemic crystals. Several studies have shown that an excess of one of the two enantiomers in the mixture of small molecules can stimulate a preferential asymmetric crystallization.[27−30] The purpose of this communication is to demonstrate that synthetic polymers can exhibit the same behavior. More specifically, we report the difference in morphology of ultrathin (thickness = 20 and 50 nm) films of mixtures of PLLA and PDLA having different enantiomeric ratios. We will show that the equimolar polylactide stereocomplex (equal quantities of PLLA and PDLA) exhibits a hexagonal crystal shape that becomes triangular for the nonequimolar mixtures (with an excess of PLLA or PDLA). Moreover, the primary and secondary branches of the dendritic crystals, obtained at thicknesses of 20 nm, exhibit a circular crystallization mode, clockwise when PDLA is in excess and counter-clockwise when PLLA is in excess. In contrast, in the hexagonal dendritic crystal, the primary and secondary branches grow linearly.

Experimental Part. *Materials.* Poly(L-lactide) was provided by Polyscience and poly(D-lactide) was provided by Purac; both were used without further purification. Their molecular weights were determined by gel permeation chromatography using a Wyatt light scattering detector: M_n = 120 000 g·mol^{-1} and polydispersity (PD) = 1.30 for PDLA; M_n = 110 000 g·mol^{-1} and PD = 1.26 for PLLA. Glass-transition temperatures and melting points were determined using a Perkin-Elmer DSC-7 apparatus. For PLLA, T_g = 57 °C and T_f (maximum of the peak, after quenching and at a scan rate of 10 °C/min) = 176 °C; for PDLA, T_g = 56 °C and T_f = 180 °C (under the same conditions as for PLLA).

Sample Preparation. Ultrathin films were prepared by spin coating at a rotation speed of 3000 rpm during 20 s, following an acceleration of 4000 rpm/s using a Headway Research EC-101 apparatus. The mass ratio of the two polyenantiomers in the film was controlled by their ratio in a dichloromethane solution. The film thickness was dictated by the solution concentration (from 1 to 20 mg/mL were used to obtain thicknesses ranging between 5 and 100 nm); for example, thicknesses of 20 and 50 nm were obtained with concentrations of 4.5 and 8 mg/mL, respectively. Films were cast onto cleaned Si substrates (p-type single side polished (100) silicon wafers) for the microscopy observations. The wafers were cleaned by immersion in nitrohydrochloric acid for 1 h in an ultrasonic bath to remove any organic contamination and to hydroxylate the native oxide layer, thus making the surface hydrophilic; they were then rinsed with distilled water and dried by spin coating for 40 s at 3000 rpm before treatment in a plasma cleaner (Harrick PDC-32G) at 18 W for 20 s. To keep a solvent-saturated atmosphere around the sample and to allow an uniform evaporation, a glass dome was placed on top of the sample area during spin coating. Film thicknesses were measured by atomic force microscopy.

Atomic Force Microscopy (AFM). A Nanoscope III Multimode AFM apparatus (Digital Instrument (DI)), operated in tapping mode and equipped with a high-temperature heating accessory (DI), was used with a JVH scanner

*Corresponding author. E-mail: re.prudhomme@umontreal.ca.

 Published on Web 04/07/2010

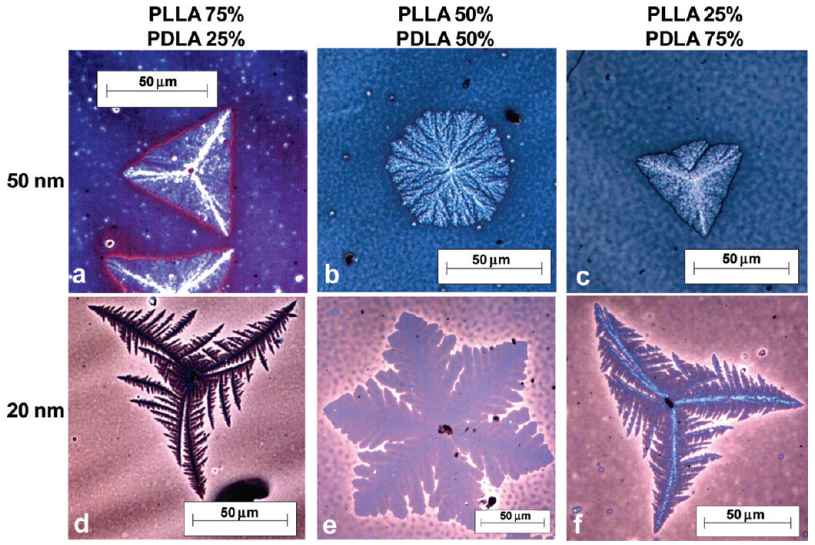

Figure 1. Optical microscopy micrographs of various PLLA/PDLA films (composition given at the top) crystallized at 200 °C. The film thickness is (a,b,c) 50 and (d,e,f) 20 nm.

(maximum scan size: 130 × 130 μm) and silicon nitride probes (Arrow NCR, reflex coated, from Nanoworld). Spin-coated samples, previously divided into small squared areas, were melted in the AFM stage at 245 °C for 2 min, and the temperature was then decreased to 200 °C. The sample surface was observed during the crystallization at a scan size of 50 × 50 μm and zoomed to observe more accurately some details. During the whole process, the AFM probe was maintained at the same temperature as the sample to avoid any condensation. The scan rate was 1 Hz, and the pictures were formed from 256 lines. Height, amplitude, and phase images were collected simultaneously. Each sample was used only once at one temperature.

Polarized Optical Microscopy (*POM*). An Axioskop-40 microscope from Carl Zeiss, equipped with 10, 20, 50, and 100× objectives and a reflection column, was used. Pictures were taken with a Micropublisher 3.3 camera from Q-Imaging and analyzed with the Image-Pro Plus 5.1 software. The contrast was enhanced by the deposition of a carbon film on the surface of the ultrathin films (108 carbon/A, Cressington Carbon Coater). The polarizers were always kept perpendicular.

Results and Discussion. Figure 1 shows optical microscopy pictures of crystals obtained from ultrathin films (20 and 50 nm) of PLLA/PDLA blends crystallized at 200 °C. At this temperature, the two polyenantiomers cannot crystallize separately, and the structures observed necessarily belong to the stereocomplex. At a thickness of 50 nm (Figure 1a,c), a triangular single crystal, covered by small triangular overgrowths oriented along the same direction as the "mother" lamella, is observed. On Figure 1c, a second primary nucleus appears in the early stage of the crystallization leading to the growth of a "fourth leg" to the crystal (at the top). In those cases, the blend is nonequimolar, with PLLA in excess in Figure 1a and PDLA in excess in Figure 1c; the global triangular shape does not depend on which polymer is in excess. For an equimolar blend, at the same film thickness (Figure 1b), the structure remains hexagonal.

Those observations are in agreement with previous crystallization studies reported in the literature for the polylactide stereocomplex.[25,31] Actually, the triangular shape is not common for polymer single crystals because there is no crystalline unit cell having that shape. According to X-ray and electron diffraction measurements, which indicate a triclinic unit cell, the triangular shape can be attributed to a specific growth mechanism resulting from the coexistence of two polymers in the same crystal.[25] This mechanism considers a "layer-by-layer" build up of the crystal with alternating layers of PLLA and PDLA with two successive layers adding simultaneously like two intertwined spirals, one made of PLLA and the other of PDLA, thus avoiding the crossing of the chain folds.[31] This model seems realistic for small perfectly triangular crystals, but it becomes problematic in the case of large or dendritic crystals.

Cartier et al.[26] have proposed a new trigonal crystalline unit cell, which can be considered as a subcell, describing the same chain packing as Okihara et al.[25] but with a simpler description of the system symmetry. Moreover, they have shown that the triangular shape is only observable in the case of nonequimolar blends of the two polyenantiomers or blends of polymers with different molecular weights. For an equimolecular blend of polyenantiomers of the same molecular weight, the single crystals are hexagonal. Cartier et al. have explained this transition from hexagonal- to triangular-shaped crystals as being due to the kinetic control of the crystallization in which a change in the mobility of one the two polyenantiomers results in a change in the aggregation rate of the chain at the growth front. Reference 26 gives a complete description of this model.

Figure 1d−f shows crystals obtained from 20 nm thick films of equimolar and nonequimolar blends (PLLA/PDLA = 3/1 in Figure 1d, 1/1 in Figure 1e, and 1/3 in Figure 1f). At this thickness, the crystals are necessarily dendritic, but their overall shape remains similar to the shape of the crystals formed in thicker films: hexagonal for the equimolar blend and triangular for the nonequimolar blends. Furthermore, each branch, primary or secondary, exhibits a triangular "arrow-head" shape. Triangular overgrowths are also present along the main axis of the branches, oriented along the same directions, not visible in Figure 1 but clearly seen at higher magnification in Figure 2.

It is interesting to note that in dendritic crystals obtained from a 20 nm film of a nonequimolar blend (Figure 1d,f), the primary and secondary branches exhibit the same triangular shape. This observation is consistent with the kinetic model of Cartier et al.[26] but not with the "snail" growth model previously proposed.[31] The crystals of Figure 1 melt at

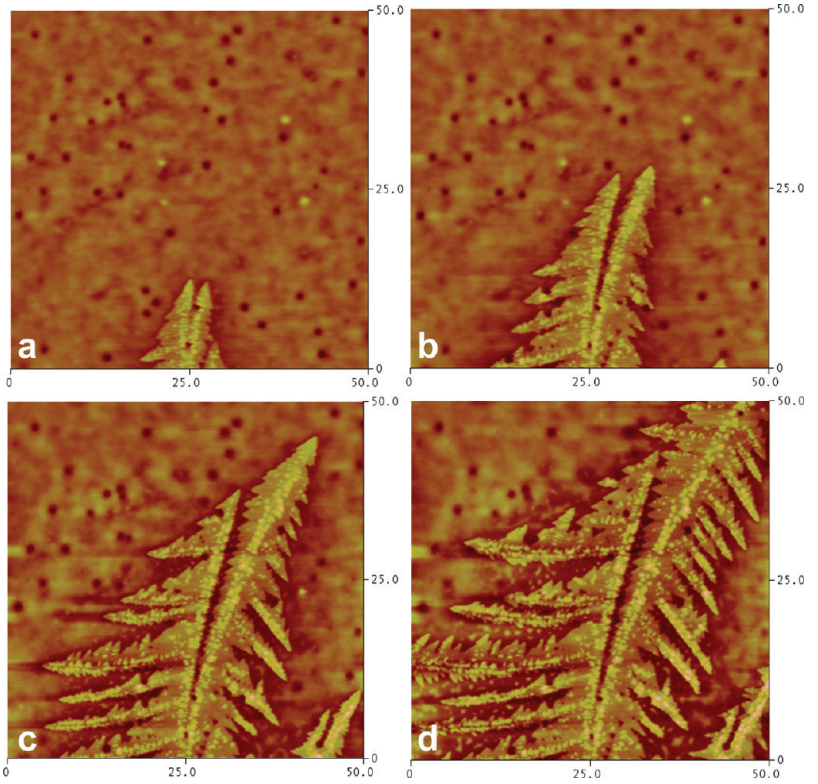

Figure 2. AFM micrographs of a PLLA/PDLA (25/75%) ultrathin film (20 nm) crystallized at 200 °C. The crystallization is followed in situ. Pictures b, c, and d were taken 21, 47, and 68 min, respectively, after picture a.

232 °C, which is in the range of the melting temperature of PLLA/PDLA stereocomplexes.[32]

Moreover, the nanometric confinement of the sample induces not only dendricity but also an overall deformation of the growth front; the dendritic crystals have concave edges (but not those in Figure 1a−c) reflecting the competition between side branches during growth. This deformation is due to the simple fact that a crystal tip (or corner in this particular case) reaches more easily the free molten polymer than a flat growth front because the dendrites result from a chain diffusion limitation at the growth front.

Finally, in the case of nonequimolar blends at a thickness of 20 nm (Figure 1d,f), the crystal branches exhibit a distortion that is dictated by the polyenantiomer in excess: the dendrites crystallize with a curvature, giving them a circularly distorted aspect. In the case of an excess of PLLA, the branches are systematically bent to the left (counterclockwise), contrary to the case of an excess of PDLA where they are bent to the right (clockwise). For an equimolecular blend (Figure 1e), the dendrites do not bend at all.

The crystallization of a 20 nm thick film of a nonequimolar PLLA/PDLA blend is followed in situ by AFM in Figure 2, with the observation of the growth of primary and secondary branches, and their curvature. Figure 2a shows the early stage of growth of the main branch and the appearance of a splitting of this branch, perhaps because of the presence of a dewetting hole on the path of its backbone. In Figure 2b, the two principal branches continue to grow, both curved to the right. Furthermore, lateral secondary branches begin to grow, but they are still too short to show any curvature. On Figure 2c, the main branches grow further and they curve, whereas the lateral secondary branches also begin to show curvatures oriented in the same direction as the main branches. Those born on the left-hand side are initially oriented at 60° from the main branch (because of the triangular architecture) but slowly curve outward the crystal during their growth; however, the branches born on the right-hand side of the mother lamella turn inward the crystal. On Figure 2d, all branches, primary and secondary, continue to grow along the same curvature pattern. From the secondary dendrites, third generation branches appear, but the lack of polymer in the surrounding does not allow them to grow. Small areas of dewetted, noncrystallized polymer are visible between the smaller branches; those areas are made of the polyenantiomer in excess (here PDLA), which has been rejected from the crystal. Because the temperature of crystallization is 20 °C above the melting temperature of the polyenantiomers taken separately, this polymer stays in the liquid phase. Furthermore, the small triangular overgrowths visible on the backbone of the branches are systematically aligned along the axis of the branches, even following their curvature.

The chiral circular distortion observed in dendritic nonequimolar crystals is unique and spectacular. Although the origin of this torsion is not perfectly understood at the present time, it can be rationalized as follows. Electron diffraction experiments, performed by us or by other groups on similar samples,[26,31] show that the unit cell remains exactly the same in the hexagonal and triangular crystals and is not affected by an excess of one of the polyenantiomers. This observation proves that the distortion is not induced by a crystalline modification. Moreover, the amorphous phase itself is not able to induce an asymmetric behavior of the crystal growth; therefore, the origin of the asymmetry must come from the intermediate phase, that is, from the chain-folding surfaces.

Contrary to the homopolymer crystals in which the chain helical rotation is the same everywhere along the crystal *c* axis (left-handed for PLLA and right-handed for PDLA), the stereocomplex crystals exhibit a structure in which half of

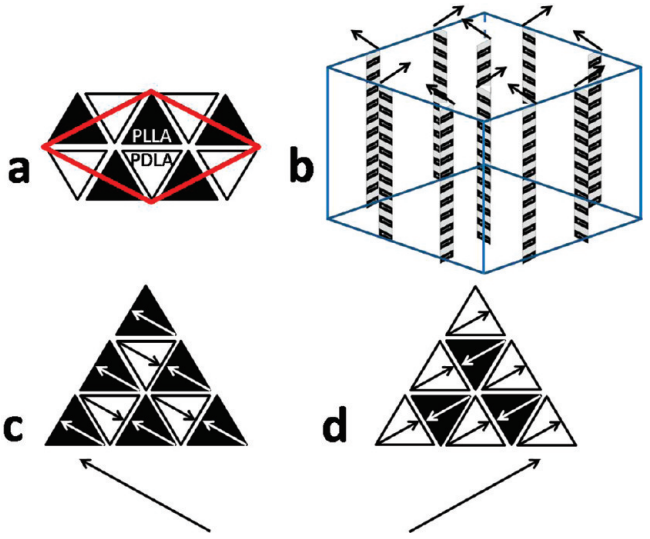

Figure 3. (A) Vertical view of the chain packing inside of the stereocomplex crystal in which the triangles represent the chains (black for PLLA, white for PDLA) due to their specific 3_1 helical conformation. The red lozenge defines the trigonal crystalline unit cell determined by Cartier and coll.[26] (B) 3D view of the trigonal unit cell in which PLLA helixes are left-handed and PDLA helixes are right-handed. The black arrows on top of the chains represent the stress due to orientation induced by the specific exit angle of each chain. The overall stress inside this unit cell is null because it contains an equal amount of PLLA and PDLA chains. (C,D) Schematic representation of the chain packing at the top tip of a triangular nonequilibrated stereocomplex crystal of PLLA- (C) or PDLA- (D) rich blends. The arrows inserted in the triangles show the stress due to orientation induced by the exit angle of each chain, and the black arrows drawn below represent the overall stress in the crystal tip.

the chains (PDLA) follow a right-handed helix and the second half (PLLA) follow a left-handed helix. Because of the symmetry of the cell, the chains exit from the crystal with a specific angle, and this angle is inverted from PLLA to PDLA. Because the chain folding naturally induces a stress on the surface of the crystal, this stress can be directionally oriented. The trigonal crystalline cell defined by Cartier et al.[26] and shown in Figure 3a contains six chains, three of each polyenantiomer. As shown in Figure 3b, the top surface is constituted of an equal number of chain exits oriented in a specific direction and chain exits in the opposite direction (direction indicated by arrows on Figure 3).

In the case of single crystals, the growth happens all along the faces of the structure but, for dendritic crystals, the growth happens at the faces close to the tip of the structure. As shown on Figure 3c,d for dendritic crystals in nonequimolar blends, at the triangular tip of the crystal, the number of the two polyenantiomers is not equal in the structure and the orientation of the chain exits becomes unbalanced. In this area, the overall stress induced by the chain exits is not compensated anymore but ruled by the polymer in excess. The stress induces a deformation of the crystal during the growth. This deformation appears here to be a bending but could also be a twisting not completely expressed due to the 2D restriction of the system. (This eventual twisting could not be observed for spherulites because it only exists under a condition of dendritic growth.) This behavior is the same at each crystal tip, not only at the three main tips (Figure 2) but also at the tips of the secondary branches; it goes in exactly opposite directions when PDLA is in excess (clockwise) or when PLLA is in excess (counterclockwise).

In summary, the crystallization of ultrathin films of polylactide blends reveals a correlation between the PLLA/PDLA ratio and the morphology of the stereocomplex crystals. The nonequimolar blend leads to triangular crystals in contrast with the hexagonal crystals observed for the equimolar blend. Moreover, for the thinnest films (20 nm) of nonequimolar blends, the triangular dendritic crystal branches exhibit a curvature, and the sense of this curvature is dictated by the polymer in excess: clockwise with an excess of PDLA and counter-clockwise with an excess of PLLA. This behavior is related to the mechanical stress occurring at the crystal tip, which can be released with a curvature of the growth direction. This is another example where ultrathin films have permitted to reveal behaviors and crystallization mechanisms that cannot be observed in thick films or in the bulk.[33]

Acknowledgment. We thank the Natural Sciences and Engineering Research Council of Canada (NSERC), the Department of Education of the Province of Québec (FQRNT program), and the Centre for Self-Assembled Chemical Structures (CSACS) for financial support. We also thank PURAC America, Inc. for providing the PDLA used. Finally, we thank Dr. Bernard Lotz, from the Institut Charles-Sadron, Strasbourg, France, for many intensive and fruitful discussions.

References and Notes

(1) Schultz, J. M.; Kinloch, D. R. *Polymer* **1969**, *10*, 271–278.
(2) Bassett, D. C.; Hodge, A. M. *Polymer* **1978**, *19*, 469–472.
(3) Singfield, K. L.; Hobbs, J. K.; Keller, A. *J. Cryst. Growth* **1998**, *183*, 683–689.
(4) Chen, Y.-F.; Woo, E. M. *Macromol. Rapid Commun.* **2009**, *30*, 1911–1916.
(5) Keith, H. D.; Padden, F. J. *J. Polym. Sci.* **1961**, *51*, S4–S7.
(6) Bassett, D. C. *Philos. Trans. R. Soc. London, Ser. A* **1994**, *348*, 29–43.
(7) Maaty, M. I. A. e.; Hosier, I. L.; Bassett, D. C. *Macromolecules* **1998**, *31*, 153–157.
(8) Xu, J.; Guo, B.; Zhang, Z.; Zhou, J.; Jiang, Y.; Yan, S.; Li, L.; Wu, Q.; Chen, G.; Schultz, J. M. *Macromolecules* **2004**, *37*, 4118–4123.
(9) Hobbs, J. K.; McMaster, T. J.; Miles, M. J.; Barham, P. J. *Polymer* **1998**, *39*, 2437–2446.
(10) Maaty, M. I. A. e.; Bassett, D. C. *Polymer* **2000**, *41*, 9169–9176.
(11) Schultz, J. M. *Polymer* **2003**, *44*, 433–441.
(12) Ho, R. M.; Ke, K. Z.; Cheng, M. *Macromolecules* **2000**, *33*, 7529–7537.
(13) Raimo, M. *J. Mater. Sci.* **2007**, *42*, 998–1003.
(14) Keith, H. D.; Padden, F. J. *Polymer* **1984**, *25*, 28–42.
(15) Lotz, B.; Cheng, S. Z. D. *Polymer* **2005**, *46*, 577–610.
(16) Bassett, D. C. *Polymer* **2006**, *47*, 3263–3266.
(17) Lotz, B.; Cheng, S. Z. D. *Polymer* **2006**, *47*, 3267–3270.
(18) Toda, A.; Hikosaka, M. *Polymer* **2001**, *42*, 2223–2233.
(19) Keith, H. D.; F. J. Padden, J.; Lotz, B.; Wittmann, J. C. *Macromolecules* **1989**, *22*, 2230–2238.
(20) Maillard, D.; Prud'homme, R. E. *Macromolecules* **2006**, *39*, 4272–4275.
(21) Maillard, D.; Prud'homme, R. E. *Macromolecules* **2008**, *41*, 1705–1712.
(22) Lotz, B.; Gonthier-Vassal, A.; Brack, A.; Magoshi, J. *J. Mol. Biol.* **1982**, *156*, 345–357.
(23) Livolant, F.; Bouligand, Y. *Chromosoma* **1980**, *80*, 97–118.
(24) Miyata, T.; Masuko, T. *Polymer* **1997**, *38*, 4003–4009.
(25) Okihara, T.; Tsuji, M.; Kawaguchi, A.; Katamaya, K. I.; Tsuji, H.; Hyon, S. H.; Ikada, Y. *J. Macromol. Sci., Part B: Phys.* **1991**, *B30*, 119–140.
(26) Cartier, L.; Okihara, T.; Lotz, B. *Macromolecules* **1997**, *30*, 6313–6322.
(27) Tamura, R.; Fujimoto, D.; Lepp, Z.; Misaki, K.; Miura, H.; Takahashi, H.; Ushio, T.; Nakai, T.; Hirotsu, K. *J. Am. Chem. Soc.* **2002**, *124*, 13153–13139.

(28) Fasel, R.; Parshau, M.; Ernst, K. H. *Angew. Chem.* **2003**, *42*, 5178–5181.
(29) Parshau, M.; Behzadi, B.; Romer, S.; Ernst, K. H. *Surf. Interface Anal.* **2006**, *38*, 1607–1610.
(30) Fasel, R.; Parschau, M.; Ernst, K. H. *Nature* **2006**, *439*, 449–452.
(31) Brizzolara, D.; Cantow, H. J.; Diedrichs, K.; Keller, E.; Domb, A. J. *Macromolecules* **1996**, *29*, 191–197.
(32) Brochu, S.; Prud'homme, R. E.; Barakat, I.; Jérôme, R. *Macromolecules* **1995**, *28*, 5230–5239.
(33) Mareau, V. H.; Prud'homme, R. E. Crystallization of Thin Polymer Films: Crystallinity, Kinetics, and Morphology. In *Soft Materials*; Dutcher, J. R., Maragoni, A. G., Eds.; Marcel Dekker, Inc.: New York, 2005; pp 39−71.